

UCSF

UC San Francisco Previously Published Works

Title

B cell-related gene signature and cancer immunotherapy response

Permalink

<https://escholarship.org/uc/item/1066646k>

Journal

British Journal of Cancer, 126(6)

ISSN

0007-0920

Authors

Lundberg, Arian

Li, Bailiang

Li, Ruijiang

Publication Date

2022-04-01

DOI

10.1038/s41416-021-01674-6

Peer reviewed

ARTICLE



Translational Therapeutics

B cell-related gene signature and cancer immunotherapy response

Arian Lundberg ^{1,2}, Bailiang Li¹ and Ruijiang Li ¹✉

© The Author(s), under exclusive licence to Springer Nature Limited 2021

BACKGROUND: B lymphocytes have multifaceted functions in the tumour microenvironment, and their prognostic role in human cancers is controversial. Here we aimed to identify tumour microenvironmental factors that influence the prognostic effects of B cells.

METHODS: We conducted a gene expression analysis of 3585 patients for whom the clinical outcome information was available. We further investigated the clinical relevance for predicting immunotherapy response.

RESULTS: We identified a novel B cell-related gene (BCR) signature consisting of nine cytokine signalling genes whose high expression could diminish the beneficial impact of B cells on patient prognosis. In triple-negative breast cancer, higher B cell abundance was associated with favourable survival only when the BCR signature was low (HR = 0.68, $p = 0.0046$). By contrast, B cell abundance had no impact on prognosis when the BCR signature was high (HR = 0.93, $p = 0.80$). This pattern was consistently observed across multiple cancer types including lung, colorectal, and melanoma. Further, the BCR signature predicted response to immune checkpoint blockade in metastatic melanoma and compared favourably with the established markers.

CONCLUSIONS: The prognostic impact of tumour-infiltrating B cells depends on the status of cytokine signalling genes, which together could predict response to cancer immunotherapy.

British Journal of Cancer (2022) 126:899–906; <https://doi.org/10.1038/s41416-021-01674-6>

INTRODUCTION

The biological and clinical relevance of T cells in antitumour immune response and immunotherapy has been well established. The role of tumour-infiltrating B cells, on the other hand, is relatively less well characterised. Recent studies have begun to reveal the multifaceted functions of B cells in the tumour microenvironment (TME) [1]. In addition to secreting antibodies and inflammatory cytokines, B cells also have the capability to present tumour antigens and modulate both innate and adaptive immune responses [2].

The prognostic role of B cells in human cancers is controversial, with conflicting results across studies [3]. While a number of studies showed a positive impact of B cells on prognosis, many others reported no impact, and a small number of studies even reported an adverse effect of B cells [3]. These differences may be attributed to the fact that B cells are a heterogeneous population with functionally distinct subsets [4], which can contribute to either pro-tumour [5] or antitumour [6] immune response. Ultimately clinical outcomes are influenced by the composition and balance among these B cell subsets, which are in turn determined by the TME milieu [7].

Several recent studies have revealed that B cells are associated with improved response and outcomes after immunotherapy [8–10]. The predictive power is stronger if B cells, together with follicular

dendritic cells and T helper cells, are located in mature tertiary lymphocyte structures (TLS), which promote B cell development and function in the germinal centre [11].

Collectively, these data support the notion that the prognostic and predictive role of tumour-infiltrating B cells is context-specific and depends on the interactions with other immune cells or factors. The purpose of this study is to systematically identify genes that regulate the prognostic effects of B cells in human cancers and investigate the clinical relevance for predicting immunotherapy response.

MATERIALS AND METHODS

Study population and data collection

The discovery cohort consists of the 10 largest breast cancer gene expression data sets that are linked with clinical outcome information. Given that triple-negative breast cancer (TNBC) has the most immune cell infiltration among all molecular subtypes, we included only TNBC samples in our analysis (META-BRCA). Three meta cohorts were generated for validation purposes, which are comprised of five non-small cell lung carcinoma (META-NSCLC), four colorectal carcinoma (META-CRC) and four melanoma (META-SKCM) data sets, respectively.

Gene expression data and clinical follow-up information were downloaded from The Cancer Genome Atlas (TCGA) [12], GEO [13] and METABRIC [14] databases. The expression value of each gene was

¹Department of Radiation Oncology, Stanford University School of Medicine, Stanford, CA, USA. ²Department of Radiation Oncology, University of California San Francisco, San Francisco, CA, USA. ✉email: rli2@stanford.edu

Received: 24 July 2021 Revised: 24 November 2021 Accepted: 9 December 2021

Published online: 17 December 2021

normalised by subtracting the mean value across all the samples in each meta cohort. Overall survival was defined as the period from the date of diagnosis or treatment initiation to the date of death or last follow-up.

Estimation for B and T lymphocytes

We used the B cell lineage abundance score (B.cell) generated by the Microenvironment Cell Populations-counter (MCP-Counter) algorithm [15] as a surrogate biomarker for B lymphocytes. The MCP-Counter uses gene expression data of the bulk tumour to calculate a score for each sample, representing an estimation of the absolute abundance of 8 immune cells and 2 non-immune stromal cell populations in the TME. Compared with other algorithms that generate a relative score for the proportions of cell populations within each sample [16], MCP-Counter could provide meaningful comparisons across different samples. We also used the T lymphocytes module (T.cell) from MCP-Counter to estimate the abundance of T lymphocytes in the TME.

A statistical model to identify genes interacting with B lymphocytes

We employed the multivariable Cox proportional hazards (Cox-PH) analyses to identify genes that interact with B lymphocytes. Specifically, we fit the following statistical model by using the *coxph* function of the *survival* package in R statistical software [17]: $hazard = \alpha \times B + \beta \times G + \gamma \times B \times G$, where the variable *B* represents the B cell abundance score for each sample and the variable *G* denotes the expression of a certain gene, while γ shows the coefficient value for the interaction effect between each gene and B cells. If the coefficient for the interaction term is statistically significant, it indicates that the corresponding gene may interact with B lymphocytes by modulating its effect on prognosis [18].

The statistical significance of the interaction was calculated using the Wald Test for each of the discovery cohorts included in META-BRCA [18]. Since the sample size of the cohorts in META-BRCA data set varied considerably, we employed Stouffer's method to generate meta *p* values. Depending on the sample size, each data set can have a higher or lower contribution in the final results, and that is reflected as weights in Stouffer's method [19]. Additionally, the meta *p* values were corrected for multiple comparisons using the Benjamini and Hochberg method (false discovery rate (FDR)) [20]. We selected the genes with $FDR < 0.1$ in the interaction test as our candidate genes.

Development of a B cell-related gene (BCR) signature

We aimed to define a gene expression signature that could regulate the prognostic effects of B cells, i.e. B cell-related gene (BCR) signature. In developing this signature, we employed several approaches to minimise false discovery rate and overfitting: i) limiting candidate genes to cytokine signalling pathways, ii) correcting for multiple testing, and iii) using correlation analysis to remove redundancy and inconsistency.

Given their important role in regulating cellular differentiation and functions, we focused our interaction analyses on the genes that are involved in cytokine signalling pathways. Here, we used a list of genes annotated in the nCounter® Human Immunology Panel Ver 2.0 (NanoString Technology, Seattle, WA). Out of the 258 genes in the panel, 163 genes were shared among all gene expression platforms and used in our analysis (Supplemental Table 1).

To remove redundancy and improve consistency, we assessed the pairwise Pearson's correlation among the candidate genes to generate a correlation matrix. Here, we conducted a meta-analysis on correlation coefficients by using *rma* function of *metafor* package in R statistical software. *rma* calculates effect sizes of the individual cohorts by applying weights to each cohort and converting them to a common metric [21]. The genes that maintained a large strength of association (65% correlation or above) with at least two other genes and clustered together were chosen as our final B cell interaction genes.

We defined a BCR signature by taking the average expression values of the final genes on an individual tumour basis. We used the Kaplan–Meier curves to demonstrate the effects of B cells on patient survival at different levels of the BCR signature. Patients were divided into B cell abundance high vs. low groups, with the median value as the cut-point. For the BCR signature, the value that corresponds to the largest difference in hazard ratios (HR) between the B cell subgroups was chosen as the threshold. In order to avoid extreme cut-points, we constrained the range of our analyses so that at least 10% of the patients were included in each group.

We tested the interaction effects of the BCR signature in independent validation cohorts for three cancer types (META-NSCLC, META-CRC, META-SKCM). In addition, we assessed the effects of B cells on patient survival at different levels of the BCR signature using cut-points defined in the same way as for the discovery cohort.

Assessment of predictive capability of BCR for immune checkpoint blockade (ICB) response

Patients of two cohorts included in META-SKCM received anti-programmed cell death protein 1 (anti-PD1) [22] and/or anti-cytotoxic T lymphocyte associated protein 4 (anti-CTLA4) [23] ICB therapies. These cohorts have publicly available gene expression profiles for 121 and 40 pre-treatment tumours with complete clinical information [22, 23]. The patient's response was assessed according to Response Evaluation Criteria in Solid Tumours (RECIST) [24]. Anti-PD1-treated patients who achieved complete response or partial response were grouped as responders, whereas patients whose disease progressed after the treatment were categorized as progressors. Patients with a mixed response ($n = 2$) or stable disease ($n = 16$) were excluded from the analyses. Anti-CTLA4-treated patients including long survival and responders, were grouped as responders, and the rest of the patients (non-responders) as progressors.

The difference between responders and progressors and their association with the BCR signature were calculated using a two-sided Student's *t*-test. We used the receiver operating characteristic (ROC) and the area under the ROC curve (AUC) to evaluate the predictive performance of the BCR signature. Furthermore, we compared the performance of BCR with several established markers of ICB response, including T.cell, a number of non-synonymous mutations in the tumours (MUT) and CD8 gene expression level [25–29]. A complete list of signatures included in this comparison is shown in Supplemental Table 2.

Lastly, we evaluated the association between BCR signature and the survival outcome of the patients who have undergone ICB treatments (anti-PD1 and/or anti-CTLA4).

Heterogeneity of B cell abundance and BCR signature across cancer types

We further investigated the heterogeneity of B cell abundance and the BCR signature among different cancer types from TCGA data by utilising the *t*-distributed Stochastic Neighbour Embedding (tSNE) map using the *tSNE* package [30] in R statistical software.

RESULTS

Patient cohorts and baseline characteristics

We collected the gene expression data and associated clinical outcome information from 23 independent studies of 4 different cancer types, leading to 4 meta cohorts. CONSORT diagrams with the exclusion criteria for this study are shown in Supplemental Fig. 1. The discovery cohort (META-BRCA) consists of 766 TNBC patients. The validation cohorts include 3 data sets (META-NSCLC, META-CRC and META-SKCM) with 1247, 1247 and 325 patients, respectively. Clinicopathological characteristics of the discovery and validation cohorts are shown in Supplemental Tables 3 and 4, respectively. A complete list of the individual patient cohorts is shown in Supplemental Table 5.

Relation between B and T lymphocytes

Given the important role of T cells in antitumour immunity, we first explored the relation between B and T lymphocytes. In META-BRCA, B cell abundance score (B.cell) and T lymphocytes module (T.cell) exhibited a relatively high correlation level (Fig. 1a, Pearson's correlation $r = 0.793$). In univariate analyses, both B.cell and T.cell were associated with a favourable prognosis in the META-BRCA cohort (Fig. 1b, HR = 0.81 and HR = 0.75, $p < 0.001$, respectively). However, in multivariate analyses, neither of them remained statistically significant (Fig. 1b, B.cell and T.cell, respectively HR = 0.90, $p = 0.30$; HR = 0.83, $p = 0.16$).

To further explore this, we stratified patients into four subgroups depending on the B cells and T cells and assessed their joint effects on prognosis, in which patients with higher

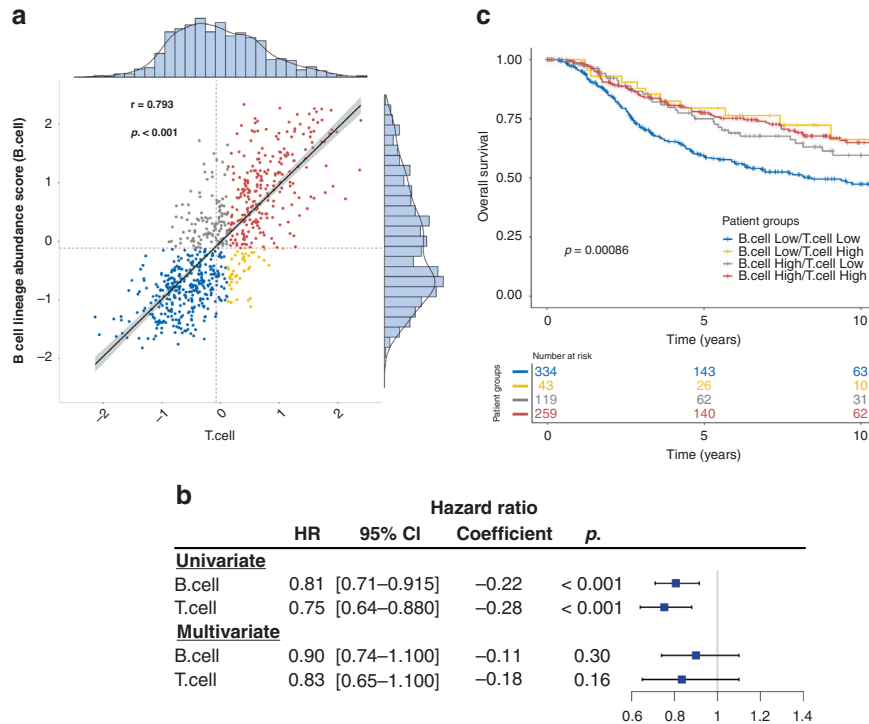


Fig. 1 Relation between B cell lineage abundance score (B.cell) and T lymphocytes module (T.cell). **a** Scatter plot showing the Pearson's correlation between B.cell and T.cell. **b** Forest plot of the univariate and multivariate analyses of B.cell and T.cell. **c** Kaplan–Meier curve representing the survival outcome of the patients with different B.cell and T.cell levels. p value refers to long-rank test. Red colour shows patients with high B.cell and T.cell; blue colour shows patients with low B.cell and T.cell; yellow colour shows patients with low B.cell and high T.cell; grey colour shows patients with high B.cell and low T.cell.

levels of both T.cell and B.cell were associated with the best survival outcome while patients with lower levels of both T.cell and B.cell showed the worst survival (Fig. 1c, $p < 0.001$); a similar trend has been observed in the validation cohorts (Supplemental Fig. 2). However, when we focussed on patient subgroups as defined by T.cell, we found that higher B.cell was associated with a better outcome only within the T.cell-low subgroup (Supplemental Fig. 3A, HR = 0.69, $p = 0.036$), while B.cell had no impact on prognosis within the T.cell-high subgroup (HR = 1.00, $p = 0.99$). This suggests that the prognostic effect of B cells may be context-specific and, in this case, is dependent on the level of T cells.

Statistical interaction analyses identify genes affecting B cells

In order to identify additional genes that may regulate the prognostic effects of B cells, we selected 163 genes involved in cytokine signalling pathways and performed statistical interaction analyses between these genes and B cell abundance in the METABRCA discovery cohort (Supplemental Table 1). In total, we found 15 genes that had a significant interaction effect (FDR < 0.1) with B cell abundance, meaning that the prognostic effect of B cells on survival outcome may be dependent on these genes (Table 1). The coefficient values derived from the interaction analyses indicate a synergistic (negative coefficient) or an antagonistic effect (positive coefficient) of these genes on B cells.

We divided the candidate genes based on their coefficient values and explored their correlation within each subgroup. The correlation matrix for the genes with an antagonistic effect and a synergistic effect on B cells were generated separately. However, the genes in the latter group showed poor consistency with a very weak correlation (Supplemental Fig. 4). Among the 11 genes with an antagonistic effect on B cells, 9 genes clustered together and maintained a relatively high level of pairwise correlation (Fig. 2a). Finally, we generated a BCR signature by taking the average

Table 1. Cytokine signalling genes interacted with B cell lineage.

Gene Symbols	ENTREZID	Coeff	p .	Adjusted p .
TRAF2	7186	0.247	0.002	0.041
TNFRSF4	7293	0.212	0.005	0.070
TNFRSF8	943	0.200	0.002	0.041
IL2RG	3561	0.198	0.006	0.070
LCK	3932	0.181	0.003	0.049
BATF	10538	0.140	0.002	0.041
TNFRSF14	8764	0.107	0.003	0.049
CXCL13	10563	0.089	0.001	0.041
IL18RAP	8807	0.045	0.002	0.041
PSMB10	5699	0.041	0.001	0.041
CXCR6	10663	0.035	0.002	0.041
IL23A	51561	-0.012	0.007	0.076
PTPN6	5777	-0.029	0.002	0.041
APP	351	-0.157	0.006	0.070
NOD1	10392	-0.174	0.006	0.070

Coeff correlation coefficient, p . p value based on Stouffer's method, Adjusted p . p value corrected for multiple comparisons using Benjamini and Hochberg method (FDR).

expression values of the 9 final genes to derive a single score for each sample.

BCR signature impacts the prognostic effect of B cells

We first examined the impact of BCR signature as a continuous variable on B cells and confirmed a significant interaction effect (HR = 1.123, $p = 0.038$, Fig. 2b). We also explored the prognostic

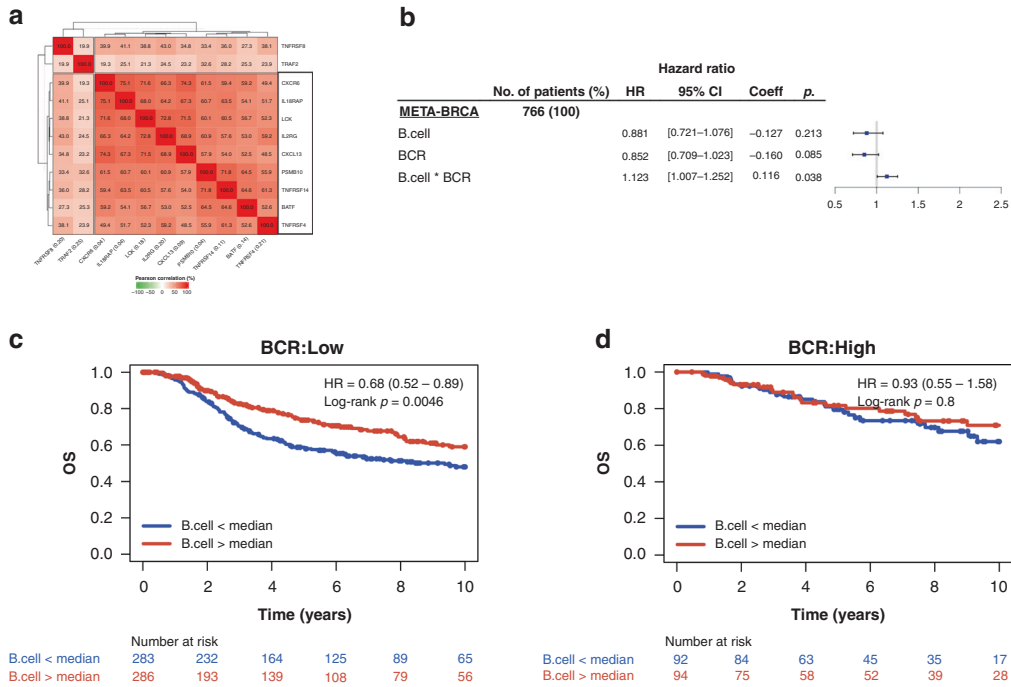


Fig. 2 Cytokine signalling genes modulating B lymphocytes prognosis. **a** Correlation matrix showing the Pearson’s correlation level (%) of genes that significantly modulate the prognostic effect of B lymphocytes; gene symbols are indicated on both axes; numbers in the parentheses represent the coefficient correlation of each gene derived from the interaction analyses. Genes with high correlation levels that are incorporated in B cell-related gene (BCR) signature are marked with a black box on the y-axis. **b** Forest plot indicating the hazard ratios of B cell lineage abundance score (B.cell) and BCR and their interaction (continuous variable) derived from Cox regression hazard models. **c, d** Kaplan–Meier curves representing survival outcome of patients in low/high BCR groups. Blue/red solid lines represent B.cell low/high within each subgroup of BCR; p values refer to log-rank test.

effect of B cells depending on the BCR signature as a binary variable. Consistently, higher B cell abundance score (B.cell) was associated with a favourable survival outcome only when the BCR signature was low (Fig. 2c, HR = 0.68, $p = 0.0046$). By contrast, B. cell was not prognostic when the BCR signature was high (Fig. 2d, HR = 0.93, $p = 0.80$). Similar results were observed for individual genes in the BCR signature (Supplemental Fig. 5).

In order to validate our findings, we chose three common cancer types that have a high level of tumour infiltrating lymphocytes including non-small cell lung carcinoma (META-NSCLC), colorectal carcinoma (META-CRC) and melanoma (META-SKCM). Similar to the discovery META-BRCA cohort, a moderate to high correlation was observed among the 9 genes in the BCR signatures in the validation cohorts (Fig. 3a, c, e, respectively).

To further investigate whether BCR captures additional biological information over T.cell, we compared both scores in the discovery and validation cohorts. Although there were some agreements between T.cell and BCR (continuous variable), this was not the case in 25.3% of META-BRCA, 24.4% of META-NSCLC, 29.3% in META-CRC and 28.9% of META-SKCM samples, respectively (data not shown).

We explored the impact of the BCR signature and B cells on patients survival. Consistent with results in the discovery cohort, higher B.cell was associated with a favourable survival outcome only within the BCR-low group but not within the BCR-high group (Fig. 3b, d, f, respectively). We then examined the prognostic impact of the BCR signature as a continuous variable on B cells, adjusted for clinical variables whenever available. Again, the BCR signature was associated with a decreased beneficial prognostic effect of B cells in META-NSCLC (HR = 1.048, $p = 0.020$), META-CRC (HR = 1.144, $p = 0.007$) and META-SKCM (HR = 1.001, $p = 0.021$) as shown in Fig. 3g. Overall, these results suggest that the prognostic effect of B cells across several cancers could be altered by the BCR genes and signature.

BCR signature predicts ICB response

Because overexpression of the BCR genes reduces the positive prognostic impact of B cells, with a negative effect on the antitumour immune response, we investigated whether they could predict clinical response to immunotherapies that might revert this process. For this purpose, two melanoma cohorts treated with anti-PD1 [22] and anti-CTLA4 [23] were selected, with publicly available data on tumour gene expression and patients’ clinical outcomes. In both cohorts, a higher BCR signature was associated with clinical response to ICB (Fig. 4a–d). The association between the BCR signature and original RECIST-categories for both cohorts are shown in Supplemental Fig. 6.

Further, we evaluated the performance of BCR signature for predicting ICB response. Compared with previous signatures [25–29] (Table 2 and Supplemental Table 2), the BCR signature had a better performance in terms of AUC for patients who received anti-PD1 treatment (Fig. 4e and Table 2, All patients, AUC = 0.610). In fact, BCR was the only signature in which the number of responders was significantly higher in the BCR-high relative to the BCR-low group as opposed to the other signatures (Table 2, all patients, $p = 0.038$). Although none of the signatures could select patients with better response when they received anti-PD1 treatment as first-line treatment (Ipi-naive), BCR signature was found to have the best performance in patients who received Ipiimumab prior to anti-PD1 treatment (Table 2, Ipi-treated, $p = 0.005$, AUC = 0.755). Similar results were found in the anti-CTLA4-treated cohort where the BCR signature performed better than the other signatures (Fig. 4f and Supplemental Table 2, $p = 0.024$, AUC = 0.732).

Next, we examined the association of BCR signature in patients who treated either with anti-PD1 (Supplemental Fig. 6, BCR:Low HR = 0.39, $p = 0.035$) or with anti-CTLA4 ICB treatment with the beneficial prognosis effect of B cells, (Supplemental Fig. 6, BCR: Low, HR = 0.40, $p = 0.042$) and indeed, BCR diminished the effect.

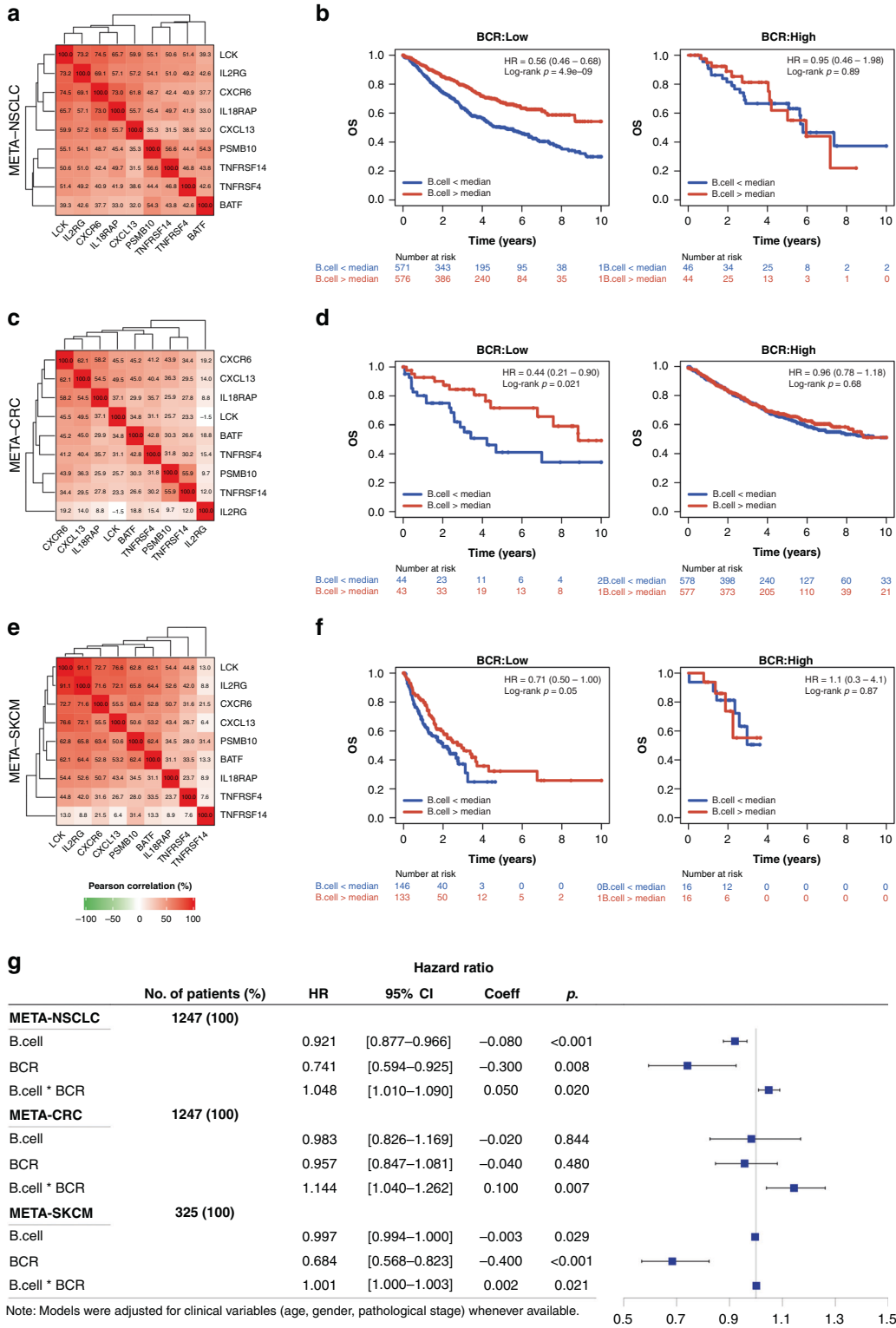


Fig. 3 Survival analysis of B cell-related gene (BCR) signature in the validation cohorts. Correlation matrices showing the Pearson's correlation level (%) between the genes that significantly modulate the prognostic effect of B lymphocytes in the validation cohorts, including **a** META-NSCLC, **c** META-CRC and **e** META-SKCM. Kaplan–Meier curves representing survival outcome of patients in low/high BCR groups in the validation cohorts, including **b** META-NSCLC, **d** META-CRC, and **f** META-SKCM. Blue/red solid lines represent B cell lineage abundance score (B.cell) low/high within each subgroup of BCR; p values refer to log-rank test. **g** Forest plot indicating the hazard ratios (HR) of B.cell and BCR (continuous variable) interaction analyses in the validation cohorts.

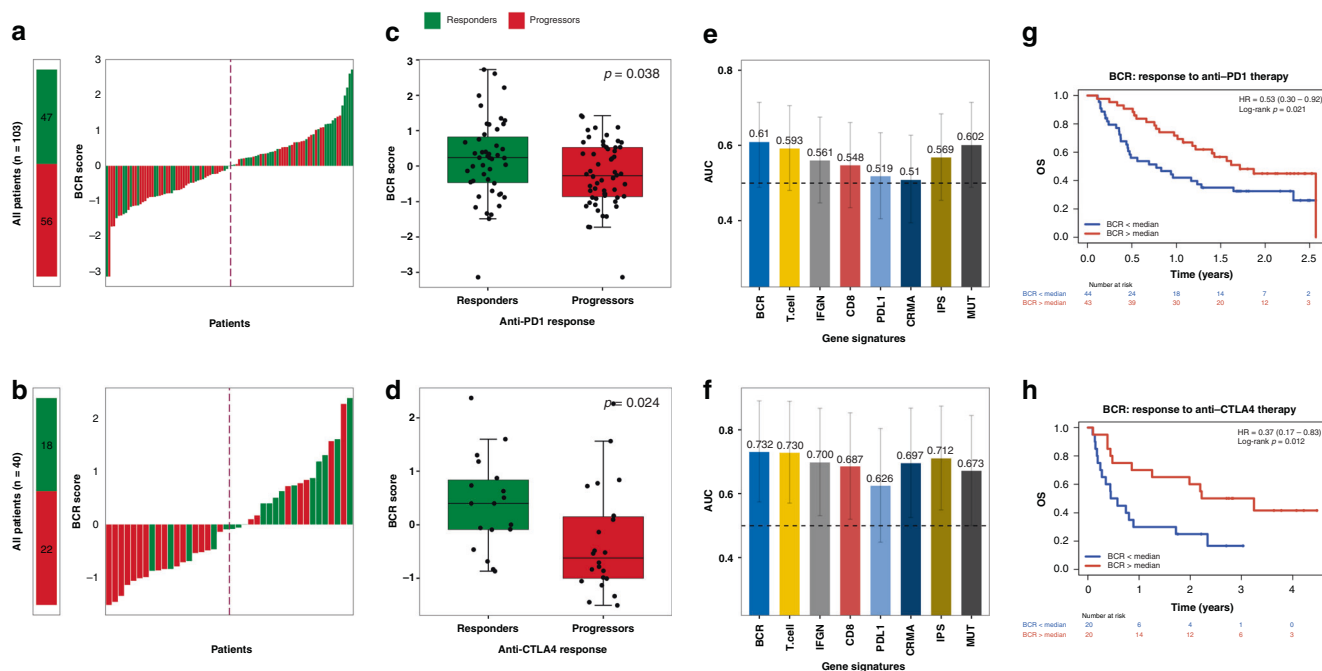


Fig. 4 B cell-related gene (BCR) signature association with anti-PD1 and anti-CTLA4 immune checkpoint blockade response. Waterfall plots of BCR prediction score across melanoma tumours treated with **a** anti-PD1 and **b** anti-CTLA4 immune checkpoint blockade (ICB). The BCR divided tumours into BCR-high (>median) or BCR-low (<median) categories. Green indicates tumours that responded to therapy (responders). Red indicates non-responders (progressors). Boxplots showing the proportion of tumours within responder or progressor groups in the **c** anti-PD1- or **d** anti-CTLA4-treated cohorts, respectively; the bottom and top of the boxes are the 25th and 75th percentiles (interquartile range); p values refer to parametric Student's t -test. Barplots indicating the predictive capability of BCR in relation to ICB response, measured by area under the ROC curve (AUC) compared to other signatures in the **e** anti-PD1- or **f** anti-CTLA4-treated cohorts, respectively; error bars represent 95% CI; Kaplan-Meier curves representing overall survival for the patients who have undergone **g** anti-PD1 or **h** anti-CTLA4 ICB treatments in the low/high (blue/red) BCR groups; p values refer to log-rank test.

Lastly, a higher BCR signature level was shown to be associated with longer survival in patients who have undergone anti-PD1 and/or anti-CTLA4 treatment (Fig. 4g— $p = 0.021$, Fig. 4h— $p = 0.012$, respectively).

BCR heterogeneity among human cancers

We conducted tSNE analyses on 9680 tumours from TCGA to estimate the heterogeneity of B.cell and BCR signature in different cancer types. We found that tumours with a higher presence of TLS such as lung adenocarcinomas show a higher level of B.cell and BCR signature, while tumours such as lower-grade glioma manifest the lowest expression of BCR signature (Supplemental Fig. 7).

DISCUSSION

B cells are increasingly being recognised as an important cell population in the TME. However, there have been inconsistent and even contradictory reports regarding the prognostic role of tumour-infiltrating B cells in human cancers. These differences are not attributable to cancer type, clinicopathologic factors, or technical approaches, suggesting that other biologic factors may be at play. In order to resolve these conflicting results, we aimed to identify tumour microenvironmental factors that influence the prognostic effects of B cells. In meta-analyses of 3585 patients across multiple cancers, we defined a novel signature consisting of 9 cytokine signalling genes whose expression in the TME correlate with a diminished beneficial prognostic impact of B cells.

The strengths of our study include the use of large patient data sets for the discovery and validation of the BCR signature. To our knowledge, no larger studies have been conducted on molecular features that specifically affect the prognostic capacity of B lymphocytes in human cancers. We employed a statistical

interaction methodology to investigate the dual role of B cells in the TME. Jiang et al. used a similar strategy to identify gene signatures of T cell dysfunction [25] while our study gave a deeper insight into the biological processes that influence the prognostic effect of B cells.

Focusing on the genes incorporated in the BCR signature revealed their complex functions in relation to the immune cells. BATF and TNFRSF14 may be both positively and negatively associated with cancer progression. BATF expression is required for differentiation of B cells and regulating CD8+ T cells [31]; on the other hand, it reduces expression of activation-induced cytidine deaminase that is essential for B cell diversification [31, 32]. TNFRSF14 gene has been shown to contribute to lymphomagenesis by interacting with B cells [33] as well as inhibition of cytokine production and proliferation of CD8+ T cells [34]. Conversely, TNFRSF14 has also been shown to suppress tumour growth with a direct impact on cancer cell apoptosis [35, 36].

Previous studies have shown that the presence of tumour-infiltrating B cells and T cells correlates with a better prognosis, suggesting the synergistic effects between the two [11, 37, 38]. Our study confirms these results, and further extends these studies by showing a context-dependent impact of B cells on prognosis. Specifically, B cells appear to play a more important role when the amount of T cells is lower, whereas B cells have no impact on survival if a larger amount of T cells is present. This result is intriguing and highlights the importance of stimulating B-cell mediated humoral immune response in order to induce an optimal adaptive antitumour immune response.

We showed that the BCR signature has the capability to predict response and outcomes in melanoma patients treated with anti-PD1 and/or anti-CTLA4 immunotherapies. The predictive performance in terms of AUC compared favourably with previously established markers. Interestingly, one of the genes in the BCR

Table 2. Assessing the predictive capability of B cell-related gene (BCR) signature regarding anti-PD1 treatments.

Gene signatures	All patients (Res: <i>n</i> = 47, Prog: <i>n</i> = 56)		Ipi-naïve (Res: <i>n</i> = 31, Prog: <i>n</i> = 33)		Ipi-treated (Res: <i>n</i> = 16, Prog: <i>n</i> = 23)	
	<i>p</i> .	AUC	<i>p</i> .	AUC	<i>p</i> .	AUC
BCR	0.038^a	0.610	0.430 ^a	0.539	0.005^a	0.755
T.cell	0.105	0.593	0.894	0.510	0.007	0.755
IFN γ	0.288	0.561	0.968	0.497	0.032	0.704
CD8	0.408	0.548	0.952	0.495	0.121	0.650
PDL1	0.738	0.519	1.000	0.500	0.301	0.601
CRMA	0.858	0.510	0.323	0.573	0.084	0.666
IPS	0.231	0.569	0.898	0.510	0.046	0.690
Mutations	0.077	0.602	0.064	0.635	0.724	0.465

All: all patients in the DFCI cohort (Liu et al.), Ipi-naïve: patients treated with first-line anti-PD1 treatment; Ipi-treated: patients treated with second-line anti-PD1 in which they were given Ipilimumab as a first-line treatment; Res: patients who showed favourable response to ICB treatments; Prog: patients who showed no/non-favourable response to ICB treatments; mutations: total count of tumour's non-synonymous mutations; BCR: B cell-related gene signature, generated by using the average expression of BATF, CXCL13, CXCR6, IL18RAP, IL2RG, LCK, PSMB10, TNFRSF4, TNFRSF14; T.cell: T lymphocyte module, generated using MCP counter (Becht et al.); IFN γ : IFNG interferon gamma response biomarkers (including IFNG, STAT1, IDO1, CXCL10, CXCL9 and HLA-DRA7 genes); CD8: generated by using the average gene expression level of CD8A + CD8B; IPS (Immunophenoscore): generated by using the average of the GZMA and PRF1 gene expression level; PDL1: PD-L1 gene (CD274) expression as the immunohistochemical surrogate; CRMA: anti-CTLA4 resistance MAGE gene signature (including MAGEA2, MAGEA2B, MAGEA3, MAGEA6 and MAGEA12); *p*: *p* values calculated with two-sided Mann-Whitney Wilcoxon test.

AUC area under the receiver-operator curve.

^a*p* values calculated with two-sided Student's *t*-test.

signature (CXCL13) has been shown to predict response to ICB in urothelial cancer [39].

We explored the inter-tumour heterogeneity of BCR and B cell infiltration in the pan-cancer setting. In tSNE analyses, testicular germ cell tumours exhibited a high level of B cells supporting a previous study by Torres et al. [40]. Interestingly, pancreatic adenocarcinoma showed a low level of B cells, likely due to the higher fibrotic stroma which may restrict the development of TLS [41]. Overall, this analysis revealed the heterogeneity of B cell infiltration and its regulator, BCR signature both within and among different cancer types.

The limitations of our study are as follows. First, our analysis is retrospective in nature. Second, we only focused on gene expression data of the bulk tumour; single-cell RNA-seq may reveal different B cell subsets with functional relevance. Third, we were not able to adjust our multivariate analyses in all meta cohorts due to the lack of clinical information in the public data sets; however, we did control for confounding factors whenever available. Finally, the genes identified in this study should be interpreted as hypothesis-generating. Future experimental studies are required to confirm their mechanistic role in regulating B cell functions in the TME.

In summary, we showed that the prognostic effect of tumour-infiltrating B lymphocytes is correlated with the status of nine cytokine signalling genes, which together could predict response to cancer immunotherapy.

DATA AVAILABILITY

All original data sets used in this article are publicly available with accession codes provided in Supplemental Table 5.

REFERENCES

- Tsou P, Katayama H, Ostrin EJ, Hanash SM. The emerging role of B cells in tumor immunity. *Cancer Res.* 2016;76:5597–601.
- Sharonov GV, Serebrovskaya EO, Yuzhakova DV, Britanova OV, Chudakov DM. B cells, plasma cells and antibody repertoires in the tumour microenvironment. *Nat Rev Immunol.* 2020;27:1–14.
- Wouters MCA, Nelson BH. Prognostic significance of tumor-infiltrating B cells and plasma cells in human cancer. *Clin Cancer Res.* 2018;24:6125–35.
- Cillo AR, Kürten CHL, Tabib T, Qi Z, Onkar S, Wang T, et al. Immune landscape of viral- and carcinogen-driven head and neck cancer. *Immunity.* 2020;52:183.e9–99.e9.
- Shalapour S, Font-Burgada J, Di Caro G, Zhong Z, Sanchez-Lopez E, Dhar D, et al. Immunosuppressive plasma cells impede T-cell-dependent immunogenic chemotherapy. *Nature.* 2015;521:94–8.
- Lu Y, Zhao Q, Liao J-Y, Song E, Xia Q, Pan J, et al. Complement signals determine opposite effects of B cells in chemotherapy-induced immunity. *Cell.* 2020;180:1081.e24–97.e24.
- Shen M, Sun Q, Wang J, Pan W, Ren X. Positive and negative functions of B lymphocytes in tumors. *Oncotarget.* 2016;7:55828–39.
- Sautés-Fridman C, Petitprez F, Calderaro J, Fridman WH. Tertiary lymphoid structures in the era of cancer immunotherapy. *Nat Rev Cancer.* 2019;19:307–25.
- Helmink BA, Reddy SM, Gao J, Zhang S, Basar R, Thakur R, et al. B cells and tertiary lymphoid structures promote immunotherapy response. *Nature.* 2020;577:549–55.
- Gentles AJ, Newman AM, Liu CL, Bratman SV, Feng W, Kim D, et al. The prognostic landscape of genes and infiltrating immune cells across human cancers. *Nat Med.* 2015;21:938–45.
- Milne K, Köbel M, Kalloger SE, Barnes RO, Gao D, Gilks CB, et al. Systematic analysis of immune infiltrates in high-grade serous ovarian cancer reveals CD20, FoxP3 and TIA-1 as positive prognostic factors. *PLoS ONE.* 2009;4:e6412.
- Cancer Genome Atlas Research Network, Weinstein JN, Collisson EA, Mills GB, Shaw KRM, Ozenberger BA, et al. The Cancer Genome Atlas Pan-Cancer analysis project. *Nat Genet.* 2013;45:1113–20.
- Edgar R, Domrachev M, Lash AE. Gene Expression Omnibus: NCBI gene expression and hybridization array data repository. *Nucleic Acids Res.* 2002;30:207–10.
- Curtis C, Shah SP, Chin S-F, Turashvili G, Rueda OM, Dunning MJ, et al. The genomic and transcriptomic architecture of 2,000 breast tumours reveals novel subgroups. *Nature.* 2012;486:346–52.
- Becht E, Giraldo NA, Lacroix L, Buttard B, Elarouci N, Petitprez F, et al. Estimating the population abundance of tissue-infiltrating immune and stromal cell populations using gene expression. *Genome Biol.* 2016;17:218.
- Newman AM, Liu CL, Green MR, Gentles AJ, Feng W, Xu Y, et al. Robust enumeration of cell subsets from tissue expression profiles. *Nat Methods.* 2015;12:453–7.
- R Development Core Team. R: a language and environment for statistical computing. Vienna: R Foundation for Statistical Computing; 2008.
- Altman DG. *Practical statistics for medical research.* Boca Raton, FL: CRC Press; 1990. 624 p.
- Stouffer SA, Suchman EA, Devinney LC, Star SA, Williams Jr. RM. *The American soldier: adjustment during army life (studies in social psychology in World War II).* Vol. 1. Oxford: Princeton Univ. Press; 1949. xii, 599 p.
- Benjamini Y, Hochberg Y. Controlling the false discovery rate: a practical and powerful approach to multiple testing. *J R Stat Soc Ser B (Methodol).* 1995;57:289–300.
- Viechtbauer W. Conducting meta-analyses in R with the metafor package. *J Stat Softw.* 2010;36:1–48.
- Liu D, Schilling B, Liu D, Sucker A, Livingstone E, Jerby-Amon L, et al. Integrative molecular and clinical modeling of clinical outcomes to PD1 blockade in patients with metastatic melanoma. *Nat Med.* 2019;25:1916–27.
- Allen EMV, Miao D, Schilling B, Shukla SA, Blank C, Zimmer L, et al. Genomic correlates of response to CTLA-4 blockade in metastatic melanoma. *Science.* 2015;350:207–11.
- Schwartz LH, Litière S, de Vries E, Ford R, Gwyther S, Mandrekar S, et al. RECIST 1.1 – update and clarification: from the RECIST Committee. *Eur J Cancer.* 2016;62:132–7.
- Jiang P, Gu S, Pan D, Fu J, Sahu A, Hu X, et al. Signatures of T cell dysfunction and exclusion predict cancer immunotherapy response. *Nat Med.* 2018;24:1550–8.
- Ayers M, Lunceford J, Nebozhyn M, Murphy E, Loboda A, Kaufman DR, et al. IFN γ -related mRNA profile predicts clinical response to PD-1 blockade. *J Clin Invest.* 2017;127:2930–40.
- Charoentong P, Finotello F, Angelova M, Mayer C, Efremova M, Rieder D, et al. Pan-cancer immunogenomic analyses reveal genotype-immunophenotype relationships and predictors of response to checkpoint blockade. *Cell Rep.* 2017;18:248–62.
- Nishino M, Ramaiya NH, Hatabu H, Hodi FS. Monitoring immune-checkpoint blockade: response evaluation and biomarker development. *Nat Rev Clin Oncol.* 2017;14:655–68.

29. Shukla SA, Bachireddy P, Schilling B, Galonska C, Zhan Q, Bango C, et al. Cancer-germline antigen expression discriminates clinical outcome to CTLA-4 blockade. *Cell*. 2018;173:624.e8–33.e8.
30. Maaten LJP, van der, Hinton GE. Visualizing high-dimensional data using t-SNE. *J Mach Learn Res*. 2008;9:2579–605.
31. Ise W, Kohyama M, Schraml BU, Zhang T, Schwer B, Basu U, et al. Batf controls the global regulators of class switch recombination in both B and T cells. *Nat Immunol*. 2011;12:536–43.
32. Xu Z, Pone EJ, Al-Qahtani A, Park S-R, Zan H, Casali P. Regulation of aicda expression and AID activity: relevance to somatic hypermutation and class switch DNA recombination. *Crit Rev Immunol*. 2007;27:367–97.
33. Mintz MA, Felce JH, Chou MY, Mayya V, Xu Y, Shui J-W, et al. The HVEM-BTLA axis restrains T cell help to germinal center B cells and functions as a cell-extrinsic suppressor in lymphomagenesis. *Immunity*. 2019;51:310.e7–23.e7.
34. Derré L, Rivals J-P, Jandus C, Pastor S, Rimoldi D, Romero P, et al. BTLA mediates inhibition of human tumor-specific CD8+ T cells that can be partially reversed by vaccination. *J Clin Invest*. 2010;120:157–67.
35. Harrop JA, McDonnell PC, Brigham-Burke M, Lyn SD, Minton J, Tan KB, et al. Herpesvirus entry mediator ligand (HVEM-L), a novel ligand for HVEM/TR2, stimulates proliferation of T cells and inhibits HT29 cell growth. *J Biol Chem*. 1998;273:27548–56.
36. Pasero C, Barbarat B, Just-Landi S, Bernard A, Aurran-Schleinitz T, Rey J, et al. A role for HVEM, but not lymphotoxin-beta receptor, in LIGHT-induced tumor cell death and chemokine production. *Eur J Immunol*. 2009;39:2502–14.
37. Li Q, Lao X, Pan Q, Ning N, Yet J, Xu Y, et al. Adoptive transfer of tumor reactive B cells confers host T-cell immunity and tumor regression. *Clin Cancer Res*. 2011;17:4987–95.
38. Al-Shibli KI, Donnem T, Al-Saad S, Persson M, Bremnes RM, Busund L-T. Prognostic effect of epithelial and stromal lymphocyte infiltration in non-small cell lung cancer. *Clin Cancer Res*. 2008;14:5220–7.
39. Goswami S, Chen Y, Anandhan S, Szabo PM, Basu S, Blando JM, et al. ARID1A mutation plus CXCL13 expression act as combinatorial biomarkers to predict responses to immune checkpoint therapy in mUCC. *Sci Transl Med*. 2020. <https://doi.org/10.1126/scitranslmed.abc4220>.
40. Torres A, Casanova JF, Nistal M, Regadera J. Quantification of immunocompetent cells in testicular germ cell tumours. *Histopathology*. 1997;30:23–30.
41. Neesse A, Michl P, Frese KK, Feig C, Cook N, Jacobetz MA, et al. Stromal biology and therapy in pancreatic cancer. *Gut*. 2011;60:861–8.

AUTHOR CONTRIBUTIONS

AL and RL contributed to the study concept and design. AL contributed to the acquisition and analyses of data. All authors interpreted the data and did the manuscript drafting and critical revision. All authors read and approved the final manuscript.

FUNDING

This research was partially supported by the National Institutes of Health grant R01 CA222512.

COMPETING INTERESTS

The authors declare no competing interests.

ETHICS APPROVAL AND CONSENT TO PARTICIPATE

Publicly available data—not applicable.

CONSENT FOR PUBLICATION

Publicly available data—not applicable.

ADDITIONAL INFORMATION

Supplementary information The online version contains supplementary material available at <https://doi.org/10.1038/s41416-021-01674-6>.

Correspondence and requests for materials should be addressed to Ruijiang Li.

Reprints and permission information is available at <http://www.nature.com/reprints>

Publisher's note Springer Nature remains neutral with regard to jurisdictional claims in published maps and institutional affiliations.